

The Analysis of Shape-based, DWT and Zernike Moments Feature Extraction Techniques for Fastener Recognition Using 10-Fold Cross Validation Multilayer Perceptrons

N. D. Mustaffa Kamal, N. Jalil, Senior Member, IEEE and H. Hashim

Abstract—This paper presents an analysis of three feature extraction techniques which are the shape-based, Zernike moments and Discrete Wavelet Transform for fastener recognition. RGB colour features are also added to these major feature extractors to enhance the classification result. The classifier used in this experiment is back propagation neural network and the result in general is strengthened using ten-fold cross validation. The result is measured using percentage accuracy and Kappa statistics. The overall results showed that the best feature extraction techniques are Zernike moment group 3 and DWT both with added colour features.

Index Terms—back propagation neural network, discrete wavelet transform, fastener recognition, RGB colour features, shape-based features, ten-fold cross validation, Zernike moments.

I. INTRODUCTION

There are thousands of unique fasteners existed until this day. Fasteners can be in countless shape and sizes. The shape varies due to the functions of the fastener. This paper focuses on fasteners which are usually used in workshops and factories. The fasteners used in this experiment are screws, nails and rivets. Commonly, fasteners users finds it hard to differentiate different type of screw from another when the tool box is mixed up with many other type of screws. When the user installed the wrong screw, he or she may find it loose or cannot fit into the joints at all. If the wrong fastener appear to fit in the joints, the fastening may be temporary and may cause damage to the machine either causing crack to the joints when large screw is used or the fastener may falls off when the machine is running. This situation is dangerous if the wrong fastener is used on cars and planes. Thus, a reliable and fast fastener recognition is needed by using machine vision.

The first process of recognising fasteners by using machine vision is by taking the images using digital camera. Then, the image is pre-processed, the features are extracted and the fasteners are classified using artificial intelligent classifier. In this paper, the main focus is on the analysis of feature extraction techniques. This analysis will enlightens the best feature extraction method to classify the fasteners.

Similar experiment that have been carried out for fastener recognition is recognition of bolt and nut using artificial neural network by Johan and Prabuwo. These researchers used webcam to capture the image of fastener in real time. The image is grayscale, thresholded, and processed using Canny edge detector to build the boundary of the fasteners. The whole image is then normalised to 50 x 50 pixels and fed into back propagation neural network. The result from the classification process is 92% recognition [1]. Although the recognition rate is good, the image used for classification have no colour information. If there are same fastener but with different coating (different colour), the classification would be inaccurate.

Another similar recent experiment is industrial strength pipeline for recognizing fastener. First, the lighting issue during the image acquisition is fixed by using illuminant-invariant filter. Otsu's thresholding method is used to segment the image of fastener from the background. The orientation of the fastener is found by calculating the visual features of the fasteners and principle component analysis (PCA) is applied to the features. Finally, support vector machine (SVM) is used to classify the fasteners. Unfortunately, the classification result is only 50% [2].

From the drawbacks of these previous experiments, this research aims to provide rapid, reliable and precise fastener recognition system. The fastener recognition system should be able to identify multiple type of fasteners and also able to include the colour features which distinguish same fastener with different coating. The accuracy of the system needs to be high and preferable close to 100%. To achieve these targets, three different feature extraction techniques are used and compared. The techniques are Shape based, Discrete Wavelet Transform (DWT) and Zernike moment (ZM). The techniques are further enhanced by adding colour features each. To identify the best feature extraction for fastener recognition, 10-fold cross validation Multilayer Perceptron (MLP) is used.

This paper is constructed as follows; Shape-based, Discrete Wavelet Transform, Zernike moments, colour features, ten-fold cross validation and multilayer perceptron are discussed in detail in section II. Methodology is discussed in section III.

Nur Diyanah Mustaffa Kamal is a master degree student at Electrical Engineering Faculty, Univerisiti Teknologi MARA, Shah Alam, Malaysia (diyanahmustaffa@yahoo.com). This paper was submitted 14 November 2016 for review. Accepted on 30th December 2016

Nor'aini Jalil is Associate Profesor in the Faculty of Electrical Engineering, Universiti Teknologi MARA, Shah Alam, Malaysia (norain365@salam.uitm.edu.my).

Hadzli Hashim is former Associate Profesor in Faculty of Electrical Engineering, Universiti Teknologi MARA, Shah Alam, Malaysia (hadzli66@salam.uitm.edu.my).

Result and discussion is discussed in section IV and conclusion in section V.

II. RESEARCH BACKGROUND

A. Shape-based Feature Extraction Technique

The first feature extraction technique to be discussed is shape-based feature extraction. Shape-based feature extraction technique is the process of calculating and gathering numerical descriptor using visual features of the object of interest [3]. This technique recognises object by using the geometrical template that determines the standard set of shapes [4]. There are two categories of shape-based feature extraction methods which are the region and contour techniques. The first category which is the region technique count the number of pixels inside the object while the second category which is the contour technique uses the object's boundary points coordinates [5]. Examples of shape-based features are area, centroid, eccentricity and perimeter. The advantages of using this technique are the descriptor are straightforward meaning it is easy to understand and the object can be recognised efficiently [3]. The weaknesses of this technique on the other hand are if the object is poorly thresholded, the result will be inaccurate, high calculation and storage consumption when the target is described comprehensively [3].

In this research, the features used are follows;

- 1) Eccentricity: Eccentricity is basically ratio of the length between the foci of the ellipse and the region's major axis length [6].

$$Eccentricity = \sqrt{\frac{\lambda_{max}}{\lambda_{min}}} \quad (1)$$

Where λ_{max} and λ_{min} are the eigenvalues of the matrix

$$\begin{bmatrix} \mu_{2,0} & \mu_{1,1} \\ \mu_{1,1} & \mu_{0,2} \end{bmatrix} \quad (2)$$

$$\mu_{p,q} = \sum x \sum y ((x - \bar{x})^p (y - \bar{y})^q) \quad (3)$$

Where x and y are coordinate of the region and \bar{x} and \bar{y} are the centroids.

- 2) Equivalent diameter: Equivalent diameter is the diameter of circle with the same area of the fastener [7].

$$Equivalent\ Diameter = \sqrt{\frac{4A}{\pi}} \quad (4)$$

Where, A is the area of the equivalent circle of the fastener.

- 3) Convex area: The number of pixels in convex image [8].
- 4) Area: The total number of pixels of the segmented fastener.
- 5) Extent: Ratio of pixels in the fastener region to the pixels in the total bounding box.
- 6) Major axis length: Length (in pixels) of the major axis of the ellipse that has the same normalized second central moments as the region [9].
- 7) Minor axis length: Length (in pixels) of the minor axis of the ellipse that has the same normalized second central moments as the region [9].



Figure 1. The comparison between area and convex area calculation image of sample object. Image (a) shows the calculation for area and (b) shows the calculation for convex area.

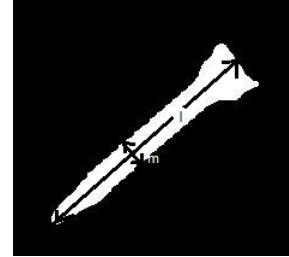


Figure 2. The major axis length(l) and minor axis length (m).

- 8) Perimeter: Number of pixels in the boundary of the foreground region [9].
- 9) Solidity: Solidity expressed how much the shape is concave or convex [10].

$$Solidity = \frac{A_s}{H} \quad (5)$$

Where, A_s is the area of fastener's region and H is the convex hull area of the foreground.

B. Discrete Wavelet Transform Feature Extraction Technique

The second feature extraction technique used in this experiment is Discrete Wavelet Transform (DWT). DWT is a mathematical approach that disintegrate a time domain signal into different frequency group. DWT is derived from Continuous Wavelet Transform (CWT) which provides time and frequency information simultaneously [11]. The advantages of DWT over CWT is it does not shift and scale endlessly due to its discrete steps nature. Other than that, DWT gives satisfactory details and lessen the computational time significantly [12]. This research will focus on two-dimensional DWT. Two dimensional DWT is the process of applying discrete wavelet transform on the rows as well as the columns of an image. Four bands are created when applying two dimensional discrete wavelet transform on the image which are the low-low (LL), low-high (LH), high-low (HL) and high-high (HH) bands [13-16]. LL band is created when low pass filter is applied to the horizontal and vertical values of the image. LH band is created when low pass filter is applied to the horizontal and high pass filter is applied to the vertical values of the image. HL band is created when high pass filter is applied to the horizontal values and low pass filter is applied to the vertical values of the image. Lastly, HH band is created when both horizontal and vertical values is filtered with high pass filter [17]. Mathematically, DWT is defined as shown in equation [11,18-20].

$$DWT(a, b) = \frac{1}{\sqrt{2^j}} \int_{-\infty}^{\infty} x(t) \psi^* \left(\frac{1-kt^j}{2^j} \right) dt \quad (6)$$

Where a and b represent 2^j and $2^j k$ respectively. 2^j is the scale parameter while $2^j k$ is the translation parameter.

The wavelet used for DWT is the most commonly used Haar wavelet [21]. Haar wavelet is used because of its low

computation needs, fast computation speed and simple to understand [22,23]. Haar wavelet is the most incomplex wavelet because of its square shaped wave [24]. Mathematically, Haar wavelet can be defined as shown in equation 7 [25]. Figure 3 shows the square-shaped Haar wavelet. Figure 4 shows input image of DWT and figure 5 shows the four sub bands created after applying DWT.

$$\psi(t) = \begin{cases} 1, 0 \leq t < \frac{1}{2} \\ -1, \frac{1}{2} \leq t < 1 \\ 0, otherwise \end{cases} \quad (7)$$

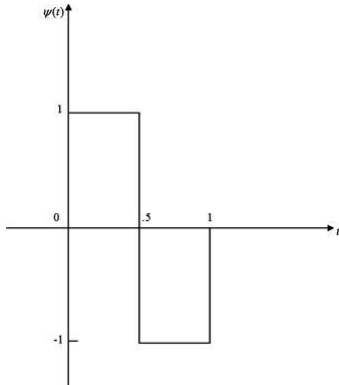


Figure 3 Haar wavelet [26].



Figure 4. Input image for DWT

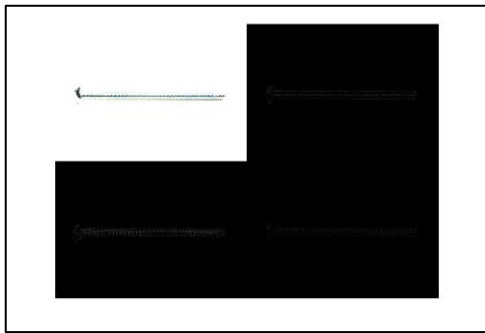


Figure 5. Four sub bands created after Haar DWT is applied to the input image.

C. Zernike Moments Feature Extraction Technique

This research also used ZM as the feature extractor for fastener recognition. ZMs are sub class of orthogonal moments [27]. Among the classes of orthogonal moments, ZM proven to be the best class because of its properties [28]. The properties are as follows;

1. Rotation invariance [28-32]
2. Robust feature descriptor [28-32]
3. Fast computation [27]
4. Multiple classes of feature descriptor for a shape [27]

5. Highly sensitive to fine details when using a high order [29]
6. Minimum information redundancy [28]

Other properties of ZM are the lower order describe the rough features and the higher order are more sensitive to noise. The higher the ZM order, the higher the computation needs, and the higher the numerical instability [28]. The fundamental definition of ZM is the plotting of image onto a set of orthogonal basis function [30] and the mathematical definition of ZM are as shown below [27,29-31].

$$A_{nm} = \frac{n+1}{\pi} \sum_{\text{over unit circle}} f(x, y) [V_{nm}(\rho, \theta)]^* \quad (8)$$

Where A_{nm} is the ZM, n is a non-negative integer, m is an integer which must satisfy the following rules,

$$n \gg 0, |m| \ll n, n - |m| = \text{even} \quad (9)$$

$f(x, y)$ is an image function with the image plotted over a unit circle and the origin is in the middle of the image. $V_{nm}(\rho, \theta)$ is defined as the Zernike polynomial where,

$$V_{nm}(x, y) = V_{nm}(\rho, \theta) = R_{nm}(\rho) e^{im\theta} \quad (10)$$

ρ is the length of vector from the middle of the image to (x, y) pixel and θ is the angle between vector ρ and the y -axis.

Radial polynomial, on the other hand, is defined as shown in equation 11.

$$R_{nm}(\rho) = \sum_{s=0}^{\frac{n-m}{2}} (-1)^s \frac{(n-s)!}{s! (\frac{n+m-s}{2})! (\frac{n-m-s}{2})!} \rho^{n-2s} \quad (11)$$

If there are pixels beyond the unit circle, the isolated pixels will not be involved in the ZM calculation [30].

D. Colour Features

Besides shape, DWT and Zernike moments features, this research also used colour features to further enhanced the classification result. Colour features used in this research is not a stand alone feature but an addition to the previous three features (shape, DWT, and Zernike moments). The colour features are extracted from RGB colour space which is the most common and oldest colour space [32,33]. RGB stands for red, green and blue colours which is the three primary colours [34,35] and can be represented in colour cube or RGB colour model as shown in figure 6 and 7. Unit colour cube use the coordinate system to define the RGB colour space. Red is placed on $(1,0,0)$, green in $(0,1,0)$, blue in $(0,0,1)$, black in $(0,0,0)$ and white in $(1,1,1)$ [35,36].

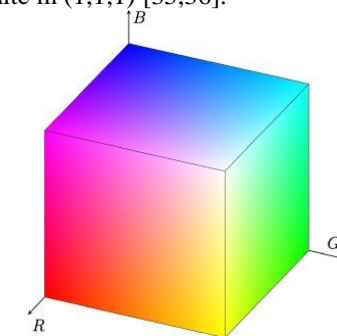


Figure 6. Unit colour cube [37].

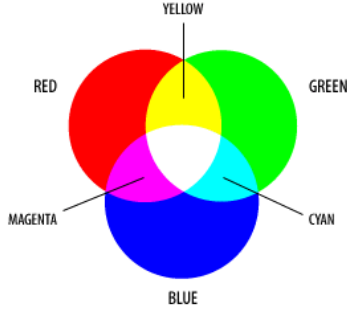


Figure 7. RGB colour model [38].

The diagonal of the cube from black's coordinate to the white coordinate is where the grey level is situated [35]. The RGB colour model on the other hand shows the resultant colour combination when red, green and blue are mixed together. With all of these colour information, colour histogram can be built to extract RGB features. Colour histogram is known as the most common tool for image classification [36] and shows the distribution of colour pixels in the image [39]. Colour histogram have axis for number of pixels and the other axis is for range of colours [39]. The advantages of colour histogram are this method is invariant to rotations, translation and scale [39].

Statistical evaluation is used to extract information from the colour histogram. Mean, standard deviation, skewedness, and kurtosis of red, green and blue channels are among the data extracted from RGB histogram. Other than that, energy and entropy of each channel are also calculated as the feature descriptors. The mean of red, green and blue channels are shown in equation 12, 13, and 14 [40].

$$Mean_{red}, \mu_R = \frac{1}{N} \sum_{(i,j)} I_R(i,j) \quad (12)$$

$$Mean_{green}, \mu_G = \frac{1}{N} \sum_{(i,j)} I_G(i,j) \quad (13)$$

$$Mean_{blue}, \mu_B = \frac{1}{N} \sum_{(i,j)} I_B(i,j) \quad (14)$$

Where, N is the number of pixels in the image channel, I_R , I_G , and I_B are the pixels of each channels for red, green and blue respectively. Standard deviation of each channels are shown in equations 15, 16 and 17 [39].

$$Std_{Red} = \sqrt{\frac{1}{N} \sum_{i=0}^N (I_R - \mu_R)^2} \quad (15)$$

$$Std_{Green} = \sqrt{\frac{1}{N} \sum_{i=0}^N (I_G - \mu_G)^2} \quad (16)$$

$$Std_{Blue} = \sqrt{\frac{1}{N} \sum_{i=0}^N (I_B - \mu_B)^2} \quad (17)$$

Skewness of each channels are shown in equations 18, 19 and 20 [41].

$$Skewness_{Red} = \frac{1}{N} \sum_{i=1}^N \left(\frac{I_{Red} - \mu_{Red}}{Std_{Red}} \right)^3 \quad (18)$$

$$Skewness_{Green} = \frac{1}{N} \sum_{i=1}^N \left(\frac{I_{Green} - \mu_{Green}}{Std_{Green}} \right)^3 \quad (19)$$

$$Skewness_{Blue} = \frac{1}{N} \sum_{i=1}^N \left(\frac{I_{Blue} - \mu_{Blue}}{Std_{Blue}} \right)^3 \quad (20)$$

Kurtosis of each channels, on the other hand, is shown in equations 21, 22, and 23 [41].

$$Kurtosis_{Red} = \frac{1}{N} \sum_{i=1}^N \left(\frac{I_{Red} - \mu_{Red}}{Std_{Red}} \right)^4 - 3 \quad (21)$$

$$Kurtosis_{Green} = \frac{1}{N} \sum_{i=1}^N \left(\frac{I_{Green} - \mu_{Green}}{Std_{Green}} \right)^4 - 3 \quad (22)$$

$$Kurtosis_{Blue} = \frac{1}{N} \sum_{i=1}^N \left(\frac{I_{Blue} - \mu_{Blue}}{Std_{Blue}} \right)^4 - 3 \quad (23)$$

Energy of each channels is shown in equation 24, 25, 26 [42].

$$Energy_{Red} = \sum_{i=1}^N |I_{Red}|^2 \quad (24)$$

$$Energy_{Green} = \sum_{i=1}^N |I_{Green}|^2 \quad (25)$$

$$Energy_{Blue} = \sum_{i=1}^N |I_{Blue}|^2 \quad (26)$$

Lastly, entropy of each channels is shown in equation 27, 28, and 29 [43].

$$Entropy_{Red} = - \sum_{i=0}^{L-1} I_{Red}(z_i) \log_2 I_{Red}(z_i) \quad (27)$$

$$Entropy_{Green} = - \sum_{i=0}^{L-1} I_{Green}(z_i) \log_2 I_{Green}(z_i) \quad (28)$$

$$Entropy_{Blue} = - \sum_{i=0}^{L-1} I_{Blue}(z_i) \log_2 I_{Blue}(z_i) \quad (29)$$

Where $I_{Red}(z_i)$, $I_{Green}(z_i)$ and $I_{Blue}(z_i)$ are the probability of red, green and blue pixels in the image respectively.

E. Back Propagation Neural Network

After all the numerical descriptors from shape-based, ZM, DWT and colours techniques are collected and arranged in systematic way, the data are fed into the classifier. The classification is carried out where the data collected are matched to the respective targets, in this case different types of fasteners. The classification is done by using back propagation neural network (BPNN). BPNN is a layered feed-forward artificial neural network where the signals are propagated forward and then the errors are sent in the opposite direction [44]. BPNN usually consist of an input layer (attributes), one or more hidden layer neurons and an output layer which consist of the targets (fasteners) [45]. The backward errors actually modifies the connection weights of the network [46]. The function of backward error propagation is to make sure the artificial neural network strongly learns the training data by reducing the error [44]. The repeated adjustment of network weights are done for a fixed number of epochs at the same time until minimum error is achieved or none at all [47]. The activation function used for all the neurons is unipolar sigmoid. Equation 30 shows the definition of unipolar sigmoid function [48]. The sigmoid function is used so that the outputs are either 0 or 1 [45].

$$S(x) = \frac{1}{1 + \frac{1}{e^x}} \quad (30)$$

F. Ten Fold Cross Validation

Ten fold cross validation originated from k-fold cross validation where it is an approach for predicting the error rate

for the classification step used [49]. The advantages of using k-fold validation are it is straightforward and this method use every data for the process of training and validation [50]. To use k-fold validation, the data needs to be separated into k sets [50]. In this research, 10 sets are created using the whole data. Nine data are used as the training set and the last data is used as the validation set [51] [52]. The process are repeated 10 times with new data for the training and validation sets [53]. Then, the accuracy are calculated using the average accuracy from the ten iterations [54]. This whole process are done to analyse the generalisation strength of the classification model [53].

III. METHODOLOGY

A. Image Acquisition & Processing

The data taken for this research are 30 different fasteners in the form of screws, nails and rivets which are usually found in Malaysia's hardware stores. All the fasteners are different in terms of shape, length, width and sizes. Some of the fasteners have distinguishly different colour from one another too. The device used for capturing images of fasteners is Canon Eos 1100D which is put on a lightbox where the individual fastener is located. The function of the lightbox is to provide a fixed lighting environment which in other word is to avoid stray lights from entering and disturbing the fixed condition. The length between the lens and the fastener is 11 cm and the angle is fixed to 90 degree. Each fastener is captured 120 times in different positions and angles. Figure 8 shows some of the fasteners image captured.



Figure 6. Sample images of fasteners captured.

The images captured are then preprocessed to lessen the computation time. Firstly, the images are rescaled by a factor of 0.3 which made the original dimension of the images changed from 2256 by 1504 pixels to 677 by 452 pixels. Then, the resized images are transform to grayscale images from RGB images. But, this step applied only for shape-based, DWT and ZM feature extraction techniques. To extract colour features, the pre-processing steps stop until the rescaling process. After the pre-processing steps is the processing step which is divided by three. The first processing steps are meant for shape-based and Zernike moments feature extraction technique. The second processing step are meant for DWT and the third processing step is for colour feature extraction technique.

1) Shape-based and Zernike moments processing steps

Here, processing steps includes removing the background, binaries, removing blobs and cropping the images automatically. The background removal is done by using Pierre Wellner's adaptive threshold method [55]. This method almost perfectly remove the background pixels. The reason for using adaptive threshold method is because most commonly used Otsu's method could not do the background

removal correctly. Otsu's method accidentally took the shadow of the image as the fastener's pixel. Figure 9 shows the difference between Otsu's method and Pierre Wellner's adaptive threshold method.

After the background is completely removed, image inversion operation is done to let the fastener image become the white pixels (value=1) and the background becomes black (value=0). Then, morphological operation is done to remove small unwanted blobs which is not from the fastener's pixels and fill the gaps and holes on the fasteners. The morphological operations includes closing, opening, and filling. Finally, the images are cropped automatically to reduce the dimension of the images. Figure 10 shows a fastener image being processed using the above steps.

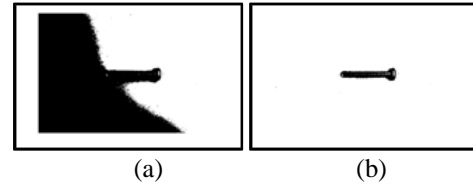


Figure 7. Comparison between (a) Otsu's threshold method and (b) Pierre Wellner's adaptive threshold method.

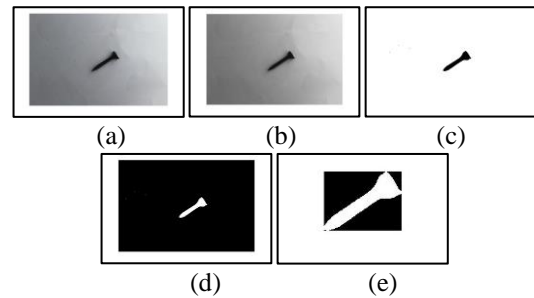


Figure 8. A fastener being processed. (a) the RGB image (b) the grayscale image (c) the thresholded image (d) the inverted image and (e) the cropped image

2) DWT processing steps

There is no processing step for DWT because the input image for the feature extraction stage are the grayscale image from the pre-processing steps.

3) RGB feature extraction processing steps

The RGB processing steps starts after the pre-processing's rescaling stage. First, the rescaled image is separated into red, green and blue colour channel. Secondly, the three images are thresholded using the Pierre Wellner's adaptive threshold method. Thirdly, the inversion operation is done to make the fastener's pixels become white which have the value of 1. Fourthly, morphological operations are applied to eliminate small blobs which are not originated from the fastener and reduce gaps as well as holes inside the fastener. The fifth step is to mask the segmented images on the rescaled images of the fastener from the pre-processing step. The resultant images produce are red, green and blue images of fastener without the background pixels.

B. Feature Extraction

Feature extraction process consists of four different parts because there are four different feature extractors. Shape-based feature extractor is done by using 'regionprops' in MATLAB R2013a directly to the segmented images of the fasteners. For Zernike moments feature extractor, orders and repetitions needs to be defined first before the calculation process. Here, the orders used are from three to seventeen. In

this research, there are three different groups of moments to define the fastener for comparison purpose. The first group is the lower order moments, the second group is the higher order moments and the third group is the combination of higher and lower order moments. Table I shows the first and second group of Zernike moments with their orders and repetitions. Thus, there are 32 moments for the first and second groups and 64 moments for the third group.

Table I: The lower and higher Zernike moments groups.

First Group : The Lower Order Moments		Second Group : The Higher Order Moments	
Orders	Repetitions	Orders	Repetitions
3	1,3	10	2,6,10
4	0,2,4	11	3,7,11
5	1,3,5	12	0,4,8,12
6	0,2,4,6	13	1,5,9,13
7	1,3,5,7	14	2,6,10,14
8	0,2,4,6,8	15	3,7,11,15
9	1,3,5,7,9	16	0,4,8,12,16
10	0,2,4,6,8,10	17	1,5,9,13,17

DWT feature extraction technique on the other hand is done by creating four sub bands from the transform. The sub bands are LL, LH, HL and HH which can be directly created using the rescaled images in the pre-processing step. The wavelet used in this research is Haar wavelet. Then, the nine numerical descriptors are calculated by using the energy of HL and HH, skewness of LH and HH, kurtosis of LH and HH, standard deviation of LH and HL and finally, entropy of LH. These numerical descriptors are used because they are proven statistically significant using Kruskal Wallis test from mean, energy, kurtosis, skewness, standard deviation and entropy of LL,LH,HL and HH. Colour feature extraction is almost the same as DWT's method which is by calculating the means, energies, skewness, kurtosis, standard deviations and entropies of red, green and blue images of fasteners. The total numerical descriptors for colour feature extraction is 18.

C. Classification

As mentioned in the research background, the classifier used is back propagation neural network by using WEKA 3.6. All the classifications have fixed parameters which is shown in Table II . The number of hidden layer used in this classifications is one and the number of nodes in the hidden layer is set to 'a'. The calculation of 'a' is shown in equation 31. The number of targets are 30 and the number of inputs depend on the classification groups. Table III shows the classification groups and inputs used. The nodes are unipolar sigmoid function. Ten fold cross validation is used during classification to see the generalisation strength of the classifier.

$$a' = \frac{\text{number of attributes} + \text{number of targets}}{2} \quad (31)$$

Table II: Parameters for BPNN for WEKA 3.6

Parameters	Chosen options
Hidden nodes	A
Learning rate	0.3
Momentum	0.2

Seed	0
Training time	500
Validation set size	0
Validation threshold	20

Table III : The classification groups' inputs.

Classification groups	Inputs	Total number of inputs
Shape-based technique	Eccentricity, equivalent diameter, convex area, area, extent, major axis length, minor axis length, perimeter and solidity.	9
Zernike group 1	32 moments	32
Zernike group 2	32 moments	32
Zernike group 3	64 moments	64
DWT	Energy of HL and HH, skewness of LH and HH, kurtosis od LH and HH, standard deviation of LH and HL and entropy of LH.	9
Colour	Mean, energy, skewness, kurtosis, standard deviaton, and entropy of red, green and blue images.	18
Shape and colour	Combination of shape and colour inputs.	27
Zernike group 1 and colour	Combination of Zernike group 1 and colour inputs	50
Zernike group 2 and colour	Combination of Zernike group 2 and colour inputs	50
Zernike group 3 and colour	Combination of Zernike group 3 and colour inputs	82
DWT and colour	Combination of DWT and colour inputs.	27

IV. RESULT & DISCUSSIONS

The objective of this research is to analyse the performance of the feature extraction techniques for fasteners recognition. The performance is done by using two measures which are the percentage of correct classification and Kappa statistics. From these measures, the best feature extraction technique can be identified scientifically. The definition of accuracy of correct classification is shown in equation 32 [56].

$$\text{Accuracy} = \frac{TN+TP}{TN+TP+FP+FN} \quad (32)$$

Where TN is true negative , TP is true positive, FN is false negative and FP is false positive.

Kappa statistics measure the degree of agreement between the model's predictions and reality [57]. The mathematical definition of Kappa statistics is shown in equation 33.

$$K = \frac{P_0 - P_c}{1 - P_c} \quad (33)$$

Where P_0 is the total agreement probability and P_c is the agreement probability which is due to chance. The range of

Kappa statistics is from negative one to positive one. Negative one shows the classification is total disagreement, zero shows random classification and positive one shows true agreement.

Table IV: Classification results

Classification groups	Correct classifications %	Kappa statistics
Shape-based technique	87.71	0.8667
Zernike group 1	41.81	0.3980
Zernike group 2	51.56	0.4989
Zernike group 3	82.11	0.8149
DWT	73.28	0.7236
Colour	98.22	0.9816
Shape-based and colour	99.72	0.9971
Zernike group 1 and colour	99.31	0.9928
Zernike group 2 and colour	99.56	0.9954
Zernike group 3 and colour	99.94	0.9994
DWT and colour	99.94	0.9994

Table IV shows the classification result using percentage of correct classification and Kappa statistics. It can be seen that the best classifications are when the colour features are added to the major feature extraction. Zernike moments, shape-based and DWT techniques alone are not sufficient for recognising fasteners. This shows that colour is an important feature which able to improve the recognition of fasteners. According to the percentage correct classification and Kappa statistics, the best classification is Zernike group 3 with colour feature (% accuracy=99.94% and Kappa statistics=0.9994) and DWT with colour feature(% accuracy=99.94% and Kappa statistics=0.9994). This followed by shape based with colour, Zernike group 2 with colour, Zernike group 1 with colour, colour alone, shape-based technique, Zernike group 3 and DWT. The most inaccurate classifications are Zernike group 1 and 2 whereby the percentage of accuracy is less than 50% and Kappa statistics less than 0.5 which signifies insufficient features for recognition.

V. CONCLUSION

In this research, the outcome of the analysis of shape-based, ZM, DWT with the addition of colour feature extraction techniques to recognise fastener have shown excellent performance. The analysis shows that the best feature extraction techniques to classify fastener are using Zernike

group 3 with and DWT both with added colour features. The worst results acquired are from ZM groups 1 and 2 where the results are insignificant. However these two groups are tested to see interms of their recognition ability using small number of features. This has proven that all the ZM features need to be utilised to acquire the best recognition. Colour features have shown to be the key to enhance other feature extraction technique and colour itself yields a good classification performance.

REFERENCES

- [1] Teuku Muhammad Johan and Anton Satria Prabuwono, "Recognition of Bolt and Nut using Artificial Neural Network," in *2011 International Conference on Pattern Analysis and Intelligent Robotics*, Putrajaya, 2011.
- [2] N. Sephus, S. Bhagavatula, P. Shastri and E. Gabriel, "An Industrial-Strength Pipeline For Recognizing Fasteners," in *2015 IEEE 14th International Conference on Machine Learning and Applications*, Atlanta, 2015.
- [3] J. Liu and Y. Shi, "Image Feature Extraction Method Based on Shape Characteristics and Its Application in Medical Image Analysis.," in *Applied Informatics and Communication International Conference*, Xian,China, 2011.
- [4] D. Yu, O. Ghita, A. Sutherland and P. F. Whelan, "A Novel Visual Speech Representation and HMM Classification For Visual Speech Recognition," in *Advances in Image and Video Technology Third Pacific Rim Symposium*, Tokyo, 2009.
- [5] A. P, M. T.T., S. S. and B. R. G., "Affine Invariant Shape Descriptor using Object Area Normalisation," in *International Conference on Power Electronics and Renewable Energy Systems (ICPERES 2014)*, Chennai, 2014.
- [6] Mokhairi Makhtar, Nur Shazwani Kamarudin, Syed Abdullah Fadzli and Mohd Fadzil Abdul Kadir, "The Contribution of Feature Selection and Morphological Operation For On-Line Business System's Image Classification," *International Journal of Multimedia and Ubiquitous Engineering*, vol. 10, no. 11, pp. 303-314, 2015.
- [7] S. Mahajan, A. Das and H. K. Sardaka, "Image acquisition techniques for assessment of legume quality," *Trends in Food Science & Technology*, no. 42, pp. 116-133, 2015.
- [8] S. Rathore, M. Hussain and A. Khan, "Automated colon cancer detection using hybrid of novel geometric features and some traditional features," *Computers in Biology and Medicine*, no. 65, p. 279-296, 2015.
- [9] B. Shrestha, Classification of Plants Using Images of Their Leaves, North Carolina: Appalachian State University, 2010.
- [10] Y. Mingqiang, K. Kpalma and J. Ronsin, "A Survey of Shape Feature Extraction Techniques," in *Pattern Recognition Techniques, Technology and Applications*, Rennes, InTech, 2008, p. 51.
- [11] J. Kim and Y. Tak, "Implementation of Discrete Wavelet Transform-based Discrimination and State-of-health Diagnosis for a Polymer Electrolyte Membrane Fuel Cell," *International Journal of Hydrogen Energy*, vol. 39, no. 20, pp. 10664-10682, 2014.
- [12] J.-D. Wu and J.-M. Koo, "An Automotive Generator Fault Diagnosis System Using Discrete Wavelet Transform and Artificial Neural Network," *Expert System with Application*, vol. 36, no. 6, pp. 9776-9783, 2009.
- [13] A. Sharma and A. Khunteta, "Satellite Image Contrast and Resolution Enhancement Using Discrete Wavelet Transform and Singular Value Decomposition," in *International Conference on Emerging Trends in Electrical, Electronics and Sustainable Energy System*, Sultanpur, 2016.
- [14] M.-J. Tsai, C.-L. Hsu, J.-S. Yin and I. Yuadi, "Digital Forensic for Printed Character Source Identification," in *IEEE International Conference on Multimedia and Expo*, Seattle, 2016.
- [15] S. G. Upase and S. V. Kuntawar, "Copy-move Detection of Image Forgery by Using DWT and SIFT Methodologist," *International Journal of Computer Applications*, vol. 149, no. 7, pp. 37-39, 2016.

- [16] H. Hu, "Variable Lighting Face Recognition Using Discrete Wavelet Transform," *Pattern Recognition Letters*, vol. 32, no. 13, pp. 1526-1534, 2011.
- [17] U. Acharya, O. Faust, S. Sreo, F. Molinari and J. S. Suri, "ThyroScreen system: High resolution ultrasound thyroid image characterization into benign and malignant classes using novel combination of texture and discrete wavelet transform," *Computer Methods and Programs in Biomedicine*, vol. 107, no. 2, pp. 233-241, 2012.
- [18] R. Kumar and M. Singh, "Outer Race Defect Width Measurement in Taper Roller Bearing Using Discrete Wavelet Transform of Vibration Signal," *Measurement*, vol. 46, no. 1, pp. 537-545, 2013.
- [19] J.-D. Wu, C.-C. Hsu and G.-Z. Wu, "Fault Gear Identification and Classification using Discrete Wavelet Transform and Adaptive Neuro-fuzzy Inference," *Expert Systems with Applications*, vol. 36, no. 3, pp. 6244-6255, 2009.
- [20] H. Ocak, "Automatic Detection of Epileptic Seizures in EEG using Discrete Wavelet Transform and Approximate Entropy," *Expert System with Applications*, vol. 36, no. 2, pp. 2027-2036, 2009.
- [21] A. Kumar, P. Rastogi and P. Srivastara, "Design and FPGA Implementation of DWR, Image Text Extraction Technique," in *3rd International Conference on Recent Trends in Computing 2015*, Ghaziabad, 2015.
- [22] R. S. Stankovic and B. J. Falkowski, "The Haar Wavelet Transform: Its Status and Achievement," *Computer and Electrical Engineering*, vol. 29, no. 1, pp. 25-44, 2003.
- [23] P. Raviraj and M. Sanavullah, "The Modified 2D-Haar Wavelet Transformation in Image Compression," *Middle-East Journal of Scientific Research*, vol. 2, no. 2, pp. 73-78, 2007.
- [24] S. Tedmori and N. Al-Najdawi, "Image Cryptographic Algorithm Based on the Haar Wavelet Transform," *Information Sciences*, vol. 269, pp. 21-34, 2014.
- [25] P. Dahal, D. Peng, Y. Yang and H. Sharif, "A Resource-Efficient Approach to Steganography in Mobile System," in *2016 International Wireless Communications and Mobile Computing Conference*, Cyprus, 2016.
- [26] N. Namazi, H. R. Burris, C. Conner and G. C. Gilbreath, "Synchronization and detection of binary data in free-space optical communication systems using Haar wavelet transformation," *Fiber Optics And Optical Communication*, vol. 45, no. 1, pp. 15001-15001, 2006.
- [27] S. M. Lajevardi and Z. M. Hussain, "Higher Order Orthogonal Moments for Invariant Facial Expression Recognition," *Digital Signal Processing*, vol. 20, no. 6, pp. 1771-1779, 2010.
- [28] C. Singh, E. Walia and N. Mittal, "Rotation invariant complex Zernike moments features and their applications to human face," *IET Computer Vision*, vol. 5, no. 5, pp. 255-266, 2011.
- [29] E. Shakeri and S. Ghaemmaghami, "An Efficient Feature Extraction Methodology for a Blind Image Steganalysis Using Contourlet Transform and Zernike Moments," in *Information Security and Cryptology 2013*, Yazd, 2013.
- [30] A. Khotanzad and H. Yaw, "Rotation Invariant Pattern Recognition Using Zernike Moments," in *9th International Conference on Pattern Recognition*, Rome, 1988.
- [31] H. Abdel Qader, A. R. Ramli and S. Al-Haddad, "Fingerprint Recognition Using Zernike Moments," *The International Arab Journal of Information Technology*, vol. 4, no. 4, pp. 372-376, 2007.
- [32] A. Manickavasagan, N. Al-Mezeini and H. Al-Shekaili, "RGB Color Imaging Technique for Grading of Dates," *Scientia Horticulturae*, vol. 175, pp. 87-94, 2014.
- [33] G. Kaur and E. Deep, "To Study Scope of Data Hiding In Various Image Color Models," *International Journal For Technological Research in Engineering*, vol. 2, no. 9, pp. 2027-2029, 2015.
- [34] Y. Zhu, H. Cheng, Z. Kun and L. Pan, "Face Detection Method Using Template Feature and Skin Color Feature in RGB Color Space," in *27th Chinese Control and Decision Conference*, Chongqing, 2015.
- [35] C. Fu-Qiang and Z. Yu-Ping, "Color Feature Extraction Of Hainan Li Brocade Image Based On RGB And HSV," in *12th International Computer Conference on Wavelet Active Media Technology and Information Processing (ICCWAMTIP)*, Chengdu, 2015.
- [36] N. Abdul Jalil, R. Sahak and A. Sapon, "Iris Localisation Using Colour Segmentation and Circular Hough Transform," in *IEEE EMBS Conference on Biomedical Engineering and Sciences*, Langkawi, 2012.
- [37] V. Chernov, J. Alander and V. Bochko, "Integer-based Accurate Conversion Between RGB and HSV Color Spaces," *Computers & Electrical Engineering*, vol. 46, pp. 328-337, 2015.
- [38] Adobe Systems Incorporated, "Technical Guides," 2000. [Online]. Available: dba.med.sc.edu/price/ir/Adobe_tg/models/rgbcmy.html. [Accessed 15 11 2016].
- [39] P. P. Kawathekar and K. J. Karande, "Use of Textural and Statistical Features for Analyzing Severity of Radiographic Osteoarthritis of Knee Joints," in *2015 International Conference on Information Processing*, Quebec, 2015.
- [40] J. Hu, D. Li, Q. Duan, Y. Han, G. Chen and X. Si, "Fish Species Classification by Color, Texture, and Multi-class Support Vector Machine Using Computer Vision," *Computers and Electronics in Agriculture*, vol. 88, pp. 133-140, 2012.
- [41] S. Otto and J. Denier, *An Introduction to Programming and Numerical Methods In MATLAB*, London: Springer, 2005.
- [42] J. L. Seixas, S. Barbon, C. M. Siqueira, I. F. L. Dias, A. G. Castaldin and A. Salvany, "Color Energy as a Seed Descriptor for Image Segmentation with Growing Algorithms on Skin Wound Image," in *2014 IEEE 16th International Conference on e-Health Networking, Applications and Services (Health Com)*, Natal, 2014.
- [43] E. Gopi, *Algorithm Collections for Digital Signal Processing Applications Using Matlab*, Netherlands: Springer, 2007.
- [44] A. Saxena, D. Kumarjain and A. Singh, "Hand Gesture Recognition Using an Android Device," in *Fourth International Conference on Communication Systems and Network Technologies*, Bhopal, 2014.
- [45] W. N. Wan Ibrahim, *Short-term Load Forecasting Using Neural Network*, Skudai: Fakulti Kejuruteraan Elektrik, Universiti Teknologi Malaysia, 2014.
- [46] Q. Zhou, H. Lu, L. Jia and K. Mao, "Automatic Modulation Classification With Genetic Backpropagation Neural Network," in *IEEE Congress on Evolutionary Computation*, Vancouver, 2016.
- [47] N. Indriani and R. Suhendar, "Scattered Object Recognition Using the Hu Moment Invariant and Backpropagation Neural Network," in *Third International Conference on Information and Communication Technology*, Nusa Dua, 2015.
- [48] X. Yu, S. Xiong, Y. He, W. Wong and Y. Zhao, "Research on Campus Traffic Congestion Detection Using BP Neural Network and Markov Model," *Information Security and Application*, vol. 31, pp. 54-60, 2011.
- [49] E. Gokgoz and A. Subasi, "Comparison of Decision Tree Algorithm for EMG Signal Classification using DWT," *Biomedical Signal Processing and Control*, vol. 18, pp. 138-144, 2015.
- [50] Y. Zhang, S. Wang, P. Phillips and G. Ji, "Binary PSO with Mutation Operator for Feature Selection Using Decision Tree Applied to Spam Detection," *Knowledge-based Systems*, vol. 64, pp. 22-31, 2014.
- [51] M. V. D. Gaag, T. Hoffman, M. Remijns, R. Hijman, L. Haan, B. V. Meijel, P. N. V. Harten, L. Valmaggio, M. D. Hert, A. Cuijpers and D. Wiersma, "The Five-factor Model of the Positive and Negative Syndrome Scale II : A Ten-fold Cross-Validation of a Revised Model," *Schizophrenia Research*, vol. 85, no. 1-3, pp. 280-287, 2006.
- [52] L. W. Hahn, M. D. Ritchie and J. H. Moore, "Multifactor Dimensionality Reduction Software for Detecting Gene-gene and Gene-environment Interactions," *Bioinformatics*, vol. 19, no. 3, pp. 376-382, 2003.
- [53] G. Singh and R. K. Panda, "Daily Sediment Yield Modeling with Artificial Neural Network Using 10-fold Cross Validation Method : A Small Agricultural Watershed, Kapgari, India," *International Journal of Sciences and Engineering*, vol. 4, no. 6, pp. 443-450, 2011.
- [54] H. Zhang, S. Yang, L. Guo, Y. Zhao, F. Shao and F. Cheng, "Comparisons of IsomiR Patterns and Classification Performance Using The Rank-based MANOVA and 10-fold Cross Validation," *Gene*, vol. 569, no. 1, pp. 21-26, 2015.
- [55] P. Wellner, "Technical Report : Adaptive Thresholding for the DigitalDesk," Rank Xerox Ltd, Cambridge, 1993.
- [56] C. Silva, S. M. Vieira and J. M. C. Sousa, "Fuzzy Decision Tree to Predict Readmissions in Intensive Care Unit," in *CONTROL'2014 - Proceedings of the 11th Portuguese Conference on Automatic Control*, Porto, 2014.

- [57] A. Ben-David, "Comparison of Classification Accuracy Using Cohen's Weighted Kappa," *Expert Systems with Applications*, vol. 34, no. 2, pp. 825-832, 2008.

Nur Diyanah Mustaffa Kamal received B.Eng.(Hons) in Mechatronics from Universiti Malaysia Perlis in 2015. Currently, she is pursuing her master's degree in Electrical Engineering at Universiti Teknologi MARA (UiTM) in the field of image processing. Her main research interest focuses on object recognition using machine vision and artificial neural network.

Dr Nor'aini Jalil is an associate professor at Universiti Teknologi Mara in electrical engineering faculty. Topics she mostly interested on are Zernike moments, orthogonal moments, and classification of iris region.

Dr Hadzli Hashim was a former associate professor at faculty of electrical engineering at Universiti Teknologi Mara. Topics he is mostly interested on are RGB color extraction of psoriasis lesion, medical skin disease imaging system and classification of rubber seed clones.